Pion-induced pion production in heavy-baryon chiral perturbation theory

N. Mobed,[1,*] J. Zhang,[2,†] and D. Singh[1,‡]

[1]*Department of Physics, University of Regina, Regina, Saskatchewan, Canada S4S 0A2*
[2]*Innovapost Inc., 365 March Road, Ottawa, Ontario, Canada K2K 3NS*

We study the reaction $\pi + N \rightarrow 2\pi + N$ within the framework of heavy-baryon chiral perturbation theory of chiral order three. The reaction cross section from threshold up to pion laboratory kinetic energies of 400 MeV is found to be in reasonable agreement with experimental data. A host of differential cross sections and angular correlations are also calculated and are found to be in semiquantitative agreement with the data. We find that contributions from amplitudes of chiral order three are large and play an essential role in reproducing the experimental data. Unitarity corrections arising from the imaginary parts of the loop-level Feynman diagrams are the only parameter-free predictions of the present calculations. It is found that the unitarity effects in some reaction channels are sizable. Finally, we evaluate polarization observables (asymmetries) for the transverse polarization of the proton target and find that the asymmetries are generally small ($\leqslant 0.4$) for the reaction under consideration.

I. INTRODUCTION

The reaction $\pi + N \rightarrow 2\pi + N$ is a well-known chiral process and has been the subject of a number of experimental [1–28] and theoretical investigations [29–38]. The reaction is of interest in connection with various aspects of chiral symmetry and its spontaneous breaking, including a determination of $\pi\pi$ scattering amplitudes and the study of nonlinear realizations of chiral symmetry.

Chiral perturbation theory (χPT) is the effective field theory of strong interactions at low energies. Over the past two decades, χPT has emerged as the appropriate framework for studying low energy processes involving pions, nucleons, and photons as external gauge fields. The mesonic sector of the theory has enjoyed substantial success in describing a number of important results. While being successful, the baryon sector of the theory, known as baryon chiral perturbation theory (BχPT), has posed some theoretical and phenomenological challenges. The problematic feature of the original formulation of BχPT [39,40] is that loop diagrams may contribute to lower order calculations. As a result, the unique chiral power counting scheme which is the essence of χPT formalism is ruined. The problem can be circumvented by employing the method of heavy baryon chiral perturbation theory (HBχPT) [41]. There has been some suggestions with regard to the slow convergence of HBχPT. More recently, manifestly Lorentz covariant formulations of BχPT which embody consistent power counting schemes have been introduced [42–46]. These formulations may also address the question of slow convergence of the chiral series. An issue, however, has been raised at the phenomenological level [47]. The majority of calculations in the baryon sector of χPT have been performed within the framework of HBχPT, and the method is still being utilized in some recent calculations [48]. The HBχPT

techniques are also currently used in the context of lattice QCD [49]. There exists a number of comprehensive reviews on the topic of χPT and its applications [50–52].

In this paper, we study the reaction $\pi + N \rightarrow 2\pi + N$ within the framework of HBχPT of chiral order three, $O(q^3)$. An extensive study of the same reaction in HBχPT of $O(q^3)$ was undertaken in Refs. [34,38]. While the overall quantitative agreement with experimental results are of similar quality in the present and previous [34,38] calculations, there are small differences between the two sets of results. We attribute these differences, in part, to the slow convergence of HBχPT series for the reaction under consideration. We will present a simple example to demonstrate that, while using equivalent Lagrangians, different truncation schemes at the Feynman diagram level result in different quantitative values for some observables. The slow convergence of HBχPT in the context of a different reaction has also been discussed in Ref. [53]. In this paper, we will also present the first calculation of polarization observables (target asymmetries) for the reaction $\pi + N \rightarrow 2\pi + N$ in HBχPT. The asymmetries have been recently measured at TRIUMF, and the data analysis is in progress [54].

This paper is organized as follows. An overview of the formalism, along with the notation employed in the present work, is given in Sec. II. Section III includes a description of the calculations and the results obtained for the reaction cross sections, differential cross sections, angular correlations, asymmetries, threshold amplitudes, and the threshold unitarity effects. An example illustrating consequences of different truncation schemes in HBχPT is discussed in Sec. IV. The summary and conclusions are presented in Sec. V.

II. FORMALISM

There are comprehensive reviews on HBχPT in the literature [50–52]. In this section, we will briefly specify our notation along with the procedure employed. The essential idea in HBχPT is that, by performing a heavy-field transformation, the nucleon mass is shifted from the propagator to the denominator of relevant interaction vertices in the effective

―――――
*Electronic address: nader.mobed@uregina.ca
†Electronic address: jingbo.zhang@innovapost.com
‡Electronic address: singhd@uregina.ca

chiral Lagrangian. The resulting Lagrangian is generally referred to as the HBχPT Lagrangian.

The heavy-field transformation can be written as

$$N_v(x) = e^{iMv_\mu x^\mu} P_v^+ \psi(x), \tag{1}$$

$$P_v^+ = \tfrac{1}{2}(1 + \not v), \quad v^2 = 1, \tag{2}$$

where v^μ is a time-like velocity four-vector, P_v^+ is a projection operator, M is the nucleon mass, ψ is the nucleon's Dirac field, and N_v is the velocity-dependent heavy-field representing a nucleon in HBχPT. The building blocks of the HBχPT Lagrangian have well defined chiral transformation properties. In the absence of external fields and in the isospin symmetric limit, the relevant quantities are

$$\chi = (m_u + m_d)B_0 = m_\pi^2, \qquad \chi_\pm = u^\dagger \chi u^\dagger \pm u \chi^\dagger u, \tag{3}$$

$$u_\mu = i(u^\dagger \partial_\mu u - u \partial_\mu u^\dagger), \qquad \nabla_\mu = \partial_\mu + \Gamma_\mu, \tag{4}$$

$$\Gamma_\mu = \tfrac{1}{2}(u^\dagger \partial_\mu u + u \partial_\mu u^\dagger),$$

where $U = u^2$ is an SU(2) valued matrix containing the pion isotriplet field for which we employ the representation

$$U = e^{i\boldsymbol{\tau} \cdot \boldsymbol{\pi}/F}, \tag{5}$$

where F is the pion decay constant and $\boldsymbol{\pi}(x)$ denotes the pion isotriplet field. Also appearing in the formalism is the so-called spin operator, given by

$$S^\mu = \frac{i}{2}\gamma_5 \sigma^{\mu\nu} v_\nu. \tag{6}$$

A. The Lagrangian

The most general chiral-invariant effective Lagrangian for the πN system is given by

$$\mathcal{L}_{\text{eff}} = \mathcal{L}_\pi + \mathcal{L}_{\pi N}, \tag{7}$$

$$\mathcal{L}_\pi = \mathcal{L}_\pi^{(2)} + \mathcal{L}_\pi^{(4)} + \dots, \tag{8}$$

$$\mathcal{L}_{\pi N} = \mathcal{L}_{\pi N}^{(1)} + \mathcal{L}_{\pi N}^{(2)} + \mathcal{L}_{\pi N}^{(3)} + \dots, \tag{9}$$

where the superscripts denote the chiral order. In the absence of external fields and in the isospin symmetric limit, the mesonic Lagrangians read [39]

$$\mathcal{L}_\pi^{(2)} = \frac{F^2}{4}\langle (u_\mu u^\mu) \rangle + \frac{1}{2}m_\pi^2 F^2 \langle U \rangle, \tag{10}$$

$$\mathcal{L}_\pi^{(4)} = \frac{1}{16}\{4l_1 \langle u_\mu u^\mu \rangle^2 + 4l_2 \langle u_\mu u_\nu \rangle^2 + l_3 \langle \chi_+ \rangle^2$$
$$+ 2l_4(\langle \chi_+ \rangle \langle u_\mu u^\mu \rangle + 2\langle \chi_-^2 \rangle)\}, \tag{11}$$

where $\langle \cdots \rangle$ denotes a trace in the SU(2) isospace, and the scale-independent LECs in the loop-level Lagrangian $\mathcal{L}_\pi^{(4)}$ are defined as

$$\bar{l}_i = \frac{32\pi^2}{\gamma_i}l_i - 2\ln\frac{m_\pi}{\mu}\left\{\frac{1}{d-4} - \frac{1}{2}[\ln(4\pi) + 1 + \Gamma'(1)]\right\},$$
$$(i = 1, 2, 3, 4) \tag{12}$$

with $(\gamma_1, \gamma_2, \gamma_3, \gamma_4) = (1/3, 2/3, -1/2, 2)$. In the absence of external fields and in the isospin symmetric limit, the πN

Lagrangians can be written as [55]

$$\mathcal{L}_{\pi N}^{(1)} = \bar{N}_v(iv \cdot \nabla + g_A S \cdot u)N_v, \tag{13}$$

$$\mathcal{L}_{\pi N}^{(2)} = \bar{N}_v \left\{ -\frac{1}{2M}(\nabla^2 + ig_A\{u \cdot v, S \cdot \nabla\}) + \frac{a_1}{M}\langle u \cdot u \rangle \right.$$
$$+ \frac{a_2}{M}\langle (u \cdot v)^2 \rangle + \frac{m_\pi^2 a_3}{M}\langle U + U^\dagger \rangle$$
$$\left. + \frac{ia_5}{M}\epsilon^{\mu\nu\alpha\beta}v_\alpha S_\beta u_\mu u_\nu \right\} N_v. \tag{14}$$

The chiral Lagrangian of $O(q^3)$ can be written as the sum

$$\mathcal{L}_{\pi N}^{(3)} = \mathcal{L}_{\pi N}^{(3),\text{Fixed}} + \mathcal{L}_{\pi N}^{(3),\text{CT}}, \tag{15}$$

where $\mathcal{L}_{\pi N}^{(3),\text{Fixed}}$ involves the fixed coefficients from πN Lagrangians of chiral orders one and two, whereas the counter-term Lagrangian $\mathcal{L}_{\pi N}^{(3),\text{CT}}$ is required for renormalization and involves new LECs. These Lagrangian pieces are of the form [55,56]

$$\mathcal{L}_{\pi N}^{(3),\text{Fixed}} = \frac{g_A}{8M^2}\bar{N}_v[\nabla_\mu, [\nabla^\mu, S \cdot u]]N_v$$
$$+ \frac{1}{2M^2}\bar{N}_v \left\{ -\left(a_5 - \frac{1 - 3g_A^2}{8}\right)u_\mu u_\nu \epsilon^{\mu\nu\alpha\beta}S_\beta \nabla_\alpha \right.$$
$$+ \frac{g_A}{2}S \cdot \nabla u \cdot \nabla + \left(a_2 + \frac{5g_A^2}{8}\right)\langle iu^\mu u \cdot v \rangle \nabla_\mu$$
$$\left. - \frac{g_A^2}{8}\{v \cdot u, u_\mu\}\epsilon^{\mu\nu\alpha\beta}v_\alpha S_\beta \nabla_\nu + \text{h.c.} \right\} N_v, \tag{16}$$

$$\mathcal{L}_{\pi N}^{(3),\text{CT}} = \frac{1}{(4\pi F)^2}\bar{N}_v\left(\sum_{i=1}^{23} b_i O_i\right)N_v. \tag{17}$$

The scale-independent LECs in $\mathcal{L}_{\pi N}^{(3),\text{CT}}$ are defined as

$$\tilde{b}_i = b_i - \beta_i\left\{\frac{1}{d-4} - \frac{1}{2}\left[\ln(4\pi) + 1 + \Gamma'(1)\right] + \ln\frac{m_\pi}{\mu}\right\}. \tag{18}$$

The pertinent pieces of the Lagrangian $\mathcal{L}_{\pi N}^{(3),\text{CT}}$ contributing to the reaction $\pi + N \to 2\pi + N$ are listed in Table I .[1]

B. Transition amplitudes and Feynman graphs

Consider the $\pi + N \to 2\pi + N$ reaction

$$\pi^a(q) + N(p_i) \longrightarrow \pi^b(q_1) + \pi^c(q_2) + N'(p_f), \tag{19}$$

where the superscripts a, b, and c are the pion isospin indices in the physical basis $(+, 0, -)$, and N and N' are the initial-state and final-state nucleons, respectively. In HBχPT, $p_i = Mv + l_i$ and $p_f = Mv + l_f$, where l denotes the residual nucleon momentum, M is the nucleon mass, and $M \gg l \cdot v$.

---

[1]The counterterm Lagrangian $\mathcal{L}_{\pi N}^{(3),\text{CT}}$ of Ref. [55] contains 24 terms. However, it has been shown that the operator O_4 in $\mathcal{L}_{\pi N}^{(3),\text{CT}}$ has a fixed coefficient a_2/M [56]. Thus, the number of independent terms in $\mathcal{L}_{\pi N}^{(3),\text{CT}}$ is 23. In this paper, we have moved the operator O_4 of Ref. [55] from $\mathcal{L}_{\pi N}^{(3),\text{CT}}$ to $\mathcal{L}_{\pi N}^{(3),\text{Fixed}}$.

TABLE I. Counterterms of $O(q^3)$ and their β-functions pertinent to the reaction $\pi + N \rightarrow 2\pi + N$.

i	O_i	β_i
1	$i[u_\mu, [v \cdot \nabla, u^\mu]]$	$-g_A^4/6$
2	$i[u_\mu, [\nabla^\mu, v \cdot u]]$	$-\left(1 + 5g_A^2\right)/12$
3	$i[v \cdot u, [v \cdot \nabla, v \cdot u]]$	$\left(3 + g_A^4\right)/6$
5	$iv_\lambda \epsilon^{\lambda\mu\nu\rho} \langle u_\mu u_\nu u_\rho \rangle$	0
6	$[\chi_-, v \cdot u]$	$\left(1 + 5g_A^2\right)/24$
11	$S \cdot u \langle u \cdot u \rangle$	$g_A \left(1 + 5g_A^2 + 4g_A^4\right)/2$
12	$u_\mu S_\nu \langle u^\mu u^\nu \rangle$	$g_A \left(3 - 9g_A^2 + 4g_A^4\right)/6$
13	$S \cdot u \langle (v \cdot u)^2 \rangle$	$-g_A \left(2 + g_A^2 + 2g_A^4\right)$
14	$v \cdot u S_\mu \langle u^\mu v \cdot u \rangle$	$\left(3g_A^3 + 2g_A^5\right) 3$
15	$\epsilon^{\mu\nu\rho\sigma} v_\rho S_\sigma \langle [v \cdot \nabla, u_\mu] u_\nu \rangle$	$g_A^4/3$
16	$\epsilon^{\mu\nu\rho\sigma} v_\rho S_\sigma \langle u_\mu [\nabla_\nu, v \cdot u] \rangle$	0
17	$S \cdot u \langle \chi_+ \rangle$	$\left(g_A + 2g_A^3\right)/2$
19	$iS^\mu [\nabla_\mu, \chi_-]$	0

The transition amplitude for the reaction $\pi + N \rightarrow 2\pi + N$ can be written as

$$\mathcal{T}_{fi} = \mathcal{A}_{fi} \langle N | \tau^\lambda | N' \rangle, \tag{20}$$

$$\mathcal{A}_{fi} = \bar{u}_v^{(\alpha_f)}(l_f) \mathcal{A} u_v^{(\alpha_i)}(l_i), \tag{21}$$

where $u_v^{(\alpha)}$ denotes the heavy baryon spinor. We find that the amplitude $\mathcal{A}$ can be decomposed as

$$\mathcal{A} = S_\mu A^\mu + i\epsilon_{\alpha\beta\mu\nu} v^\alpha q^\beta q_1^\mu q_2^\nu B, \tag{22}$$

$$A^\mu = A_0 q^\mu + A_1 q_1^\mu + A_2 q_2^\mu, \tag{23}$$

where A_i $(i = 0, 1, 2)$ and B are invariant functions of external momenta. The amplitudes A_i and B are obtained by adding terms of appropriate structure from all the diagrams contributing to the process under consideration. To a given chiral order, the transition amplitude $\mathcal{T}_{fi}$ receives contributions from all possible connected Feynman diagrams up to that order. The topologically distinct diagrams of up to $O(q^3)$ contributing to the reaction $\pi + N \rightarrow 2\pi + N$ are shown in Fig. 1. The self-energy graphs are not shown.

The transition amplitude $\mathcal{T}_{fi}$ can be written as a sum of the amplitudes of well-defined chiral order. Up to $O(q^3)$ one has $\mathcal{T}_{fi} = \sum_{i=1}^{3} \mathcal{T}_{fi}^{(i)}$, where the superscript (i) denotes the chiral order. The amplitudes $\mathcal{T}_{fi}^{(i)}$ of order $O(q^i)$ receive contributions from the following diagrams:

(i) The $O(q)$ graphs are the trees constructed with $\mathcal{L}_{\pi N}^{(1)}$ and $\mathcal{L}_\pi^{(2)}$.

(ii) The $O(q^2)$ graphs are the trees constructed with $\mathcal{L}_{\pi N}^{(1)}$, $\mathcal{L}_{\pi N}^{(2)}$ and $\mathcal{L}_\pi^{(2)}$.

(iii) The $O(q^3)$ graphs include three types of contributions:

    (a) the trees constructed with $\mathcal{L}_{\pi N}^{(1)}$, $\mathcal{L}_{\pi N}^{(2)}$, $\mathcal{L}_{\pi N}^{(3)}$, $\mathcal{L}_\pi^{(2)}$, and $\mathcal{L}_\pi^{(4)}$;

    (b) the loop diagrams with vertices from $\mathcal{L}_{\pi N}^{(1)}$ and $\mathcal{L}_\pi^{(2)}$;

    (c) the tree diagrams of $O(q)$ multiplied by appropriate powers of nucleon and pion renormalization constants Z_N [57] and Z_π [58] to arrive at diagrams of $O(q^3)$.
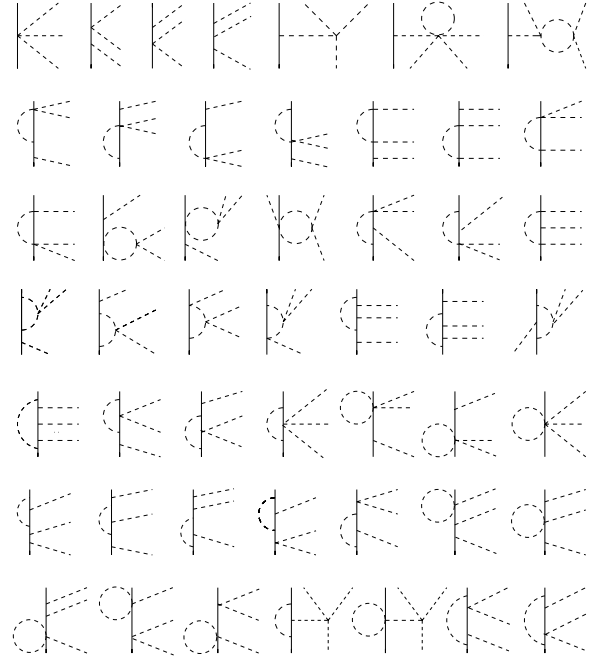

FIG. 1. Topologically distinct graphs contributing to the reaction $\pi + N \rightarrow 2\pi + N$ up to $O(q^3)$.

As a necessary check of our calculations, it was verified that the sum of the diagrams of $O(q^3)$ are free of ultraviolet divergences.

We find that loop integrals fall into the following two categories:

(i) Analytically solvable integrals involving only two pion propagators, as well as integrals involving one pion and arbitrary number of nucleon propagators;

(ii) Numerically solvable integrals involving at least one nucleon and two pion propagators.

Had it not been for the second type of integrals, the entire transition amplitude would have been expressed in closed analytical form. The explicit expressions for the one-particle irreducible Feynman diagrams, as well as the relevant loop integrals, are somewhat unwieldy. These expressions are available in Ref. [59].

III. CALCULATIONS AND RESULTS

The methodology of calculations in HBχPT is well documented [50,52]. There is a proliferation of LECs beyond $O(q^2)$ in HBχPT. In general, only a subset of LECs contribute to a given reaction. The numerical values of the LECs originating from $\mathcal{L}_{\pi N}^{(1)}$, $\mathcal{L}_{\pi N}^{(2)}$, $\mathcal{L}_\pi^{(2)}$, $\mathcal{L}_\pi^{(4)}$, and contributing to the reaction under consideration are listed in Tables II, III, and IV.

TABLE II. LECs contributing to amplitudes of $O(q)$ or higher in HBχPT [58].

F_π(MeV)	g_A
92.4 ± 0.3	1.2601 ± 0.0025

TABLE III. LECs contributing to amplitudes of $O(q^2)$ or higher in HBχPT [53].

a_1	a_2	a_3	a_5
-2.60 ± 0.03	1.40 ± 0.05	-1.00 ± 0.06	3.30 ± 0.05

TABLE V. The dimensionless LECs originating from the meson-baryon Lagrangian of chiral order $O(q^3)$ contributing to amplitudes of $O(q^3)$ or higher in HBχPT [53].

$\tilde{b}_1 + \tilde{b}_2$	$\tilde{b}_3$	$\tilde{b}_6$	$\tilde{b}_{15} - \tilde{b}_{16}$	$\tilde{b}_{19}$
2.4 ± 0.3	-2.8 ± 0.6	1.4 ± 0.3	-6.1 ± 0.4	-2.4 ± 0.2

In addition, for the reaction $\pi + N \rightarrow 2\pi + N$, there are 13 LECs originating from $\mathcal{L}_{\pi N}^{(3)}$ corresponding to different terms listed in Table I. Five relevant combinations containing seven LECs were previously determined in connection with the elastic πN scattering and the Goldberger-Treiman discrepancy. These are listed in Table V. The remaining six LECs of $O(q^3)$, $\tilde{b}_5$, $\tilde{b}_{11}$, $\tilde{b}_{12}$, $\tilde{b}_{13}$, $\tilde{b}_{14}$, $\tilde{b}_{17}$, need to be determined. We emphasize that we treat the previously determined LECs as fixed, and will attempt to determine only the unknown LECs by fitting the experimental data. There are a variety of total and differential cross sections available for the reaction $\pi + N \rightarrow 2\pi + N$. We include the total [1–25] and double differential [26,27] cross section data with $T_\pi \leqslant 250$ MeV in the fitting procedure. The kinematic range was chosen to coincide with the previous work on the same reaction for comparison [38]. Once the LECs are determined, our predictions include total cross sections with $T_\pi \geqslant 250$ MeV, invariant differential cross sections, angular correlation functions, and polarization observables. As a fitting strategy, it was initially assumed that LECs of $O(q^3)$ should be constrained to a natural size of 10 in dimensionless units. This condition proved to be too restrictive. The constraint was then relaxed and the unknown LECs were allowed to vary over a wider range. It was found that different sets of LECs can reproduce the data with a similar quality of fit, so far as χ^2/dof is concerned. To facilitate the selection of a set of LECs, the renormalization group fixed-point analysis of the LECs proposed in Ref. [60] was employed. In this method, one obtains an estimate of the ratios of the LECs which have nonvanishing beta functions. As a result, one can arrive at relations between the known and unknown LECs. This leads to estimates for the LECs $\tilde{b}_{11}$, $\tilde{b}_{12}$, $\tilde{b}_{13}$, $\tilde{b}_{14}$, $\tilde{b}_{17}$. The LEC $\tilde{b}_5$, having a vanishing beta function, cannot be estimated in this method. It is worth mentioning that, with our representation of the pion field (5), the LEC $\tilde{b}_5$ contributes only to the reaction channels involving a single neutral pion in the final state. The above-mentioned estimates of the unknown LECs with allowance for a broad range of variations were then inputted in the fitting routine. It was found that a creative use of initial estimates results in a faster convergence of the fitting routine. The set of LECs employed in present calculations are listed in Table VI.

TABLE IV. LECs originating from the mesonic Lagrangian of chiral order $O(q^4)$ contributing to amplitudes of $O(q^3)$ or higher in HBχPT [39].

$\bar{l}_1$	$\bar{l}_2$	$\bar{l}_3$	$\bar{l}_4$
-2.3 ± 3.7	6.0 ± 1.3	2.9 ± 2.4	4.3 ± 0.9

A. Total cross section

Our results for the reaction cross section in the low energy region ($T_\pi \leqslant 250$ MeV, fitting region) and in the broader kinematic range of up to $T_\pi = 400$ MeV are shown in Figs. 2 and 3, respectively. The prominent features of the results may be summarized as follows. As one moves away from the reaction threshold, the leading order calculations [calculations of $O(q)$] significantly underestimate the data. Contributions from terms of $O(q^2)$ are generally small, whereas contributions of $O(q^3)$ are large and result in a much improved agreement with experimental data. As expected, the relative contributions of nonleading terms increase with energy. One may also note that for an effective theory that is expected to work in the threshold region the overall agreement between theory and experiment at higher energies seems reasonable.

B. Differential cross section

As described above, the available low-energy double differential cross section data, $d^2\sigma/d\Omega dT$ [26,27], and the reaction cross section data were used to determine the unknown LECs of $O(q^3)$. Two samples of fitted results for $d^2\sigma/d\Omega dT$ for different kinematic conditions are shown in Fig. 4. The quality of fit to the remaining $d^2\sigma/d\Omega dT$ data is similar to what is shown in Fig. 4.

The subsequent theoretical results presented in this section can be regarded as predictions rather than fits. The sample calculations for invariant differential cross sections, $d\sigma/ds_{\pi\pi}$ and $d\sigma/dt_{\pi\pi}$, are shown in Figs. 5 and 6. The sample results for the angular correlation function $W(\theta_\pi, \phi_\pi)$ are shown in Fig. 7.

The common feature of the differential cross section calculations presented in this work is that contributions of $O(q^3)$ are large. Furthermore, to the extent that the experimental data is reproduced these contributions are essential.

C. Threshold amplitudes

HBχPT provides a systematic chiral expansion of S-matrix elements for single nucleon processes. Although the expansion is carried out in a special reference frame characterized by a time-like unit four-vector v^μ, it has been pointed out [61] that the physical observables are independent of the choice of frame due to the Lorentz invariance of the underlying meson-baryon Lagrangian.

The analysis of experimental data is often carried out in terms of the Lorentz-invariant form factors and amplitudes.

TABLE VI. LECs of chiral order $O(q^3)$ determined in this work by using the fitting procedure described in the text. The χ^2/dof of the fit is 3.4.

$\tilde{b}_5$	$\tilde{b}_{11}$	$\tilde{b}_{12}$	$\tilde{b}_{13}$	$\tilde{b}_{14}$	$\tilde{b}_{17}$
2.6 ± 3.3	-25.1 ± 6.2	-10.2 ± 4.7	22.3 ± 5.7	-8.4 ± 2.7	-5.3 ± 1.1

Therefore, it is desirable to express the invariant amplitudes in terms of the frame-dependent quantities of HBχPT. The key step in finding relationships between the two sets of amplitudes is the introduction of a matching condition. Following Ref. [61], we write the matching condition as

$$\bar{u}(p_f)\,\Gamma\,u(p_i) = \bar{u}_v(p_f)\,\hat{\Gamma}\,u_v(p_i), \qquad (24)$$
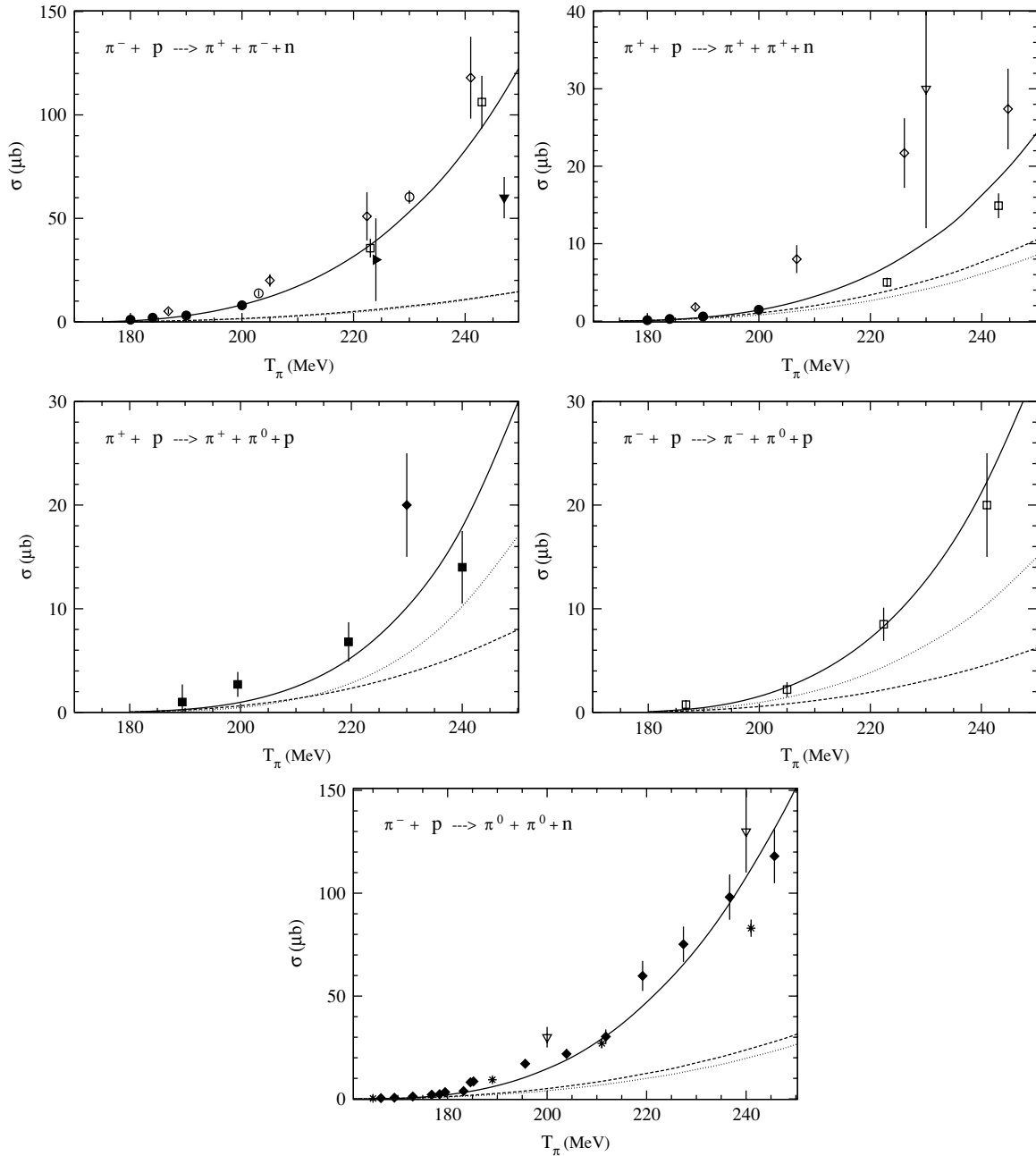

FIG. 2. Fits to total reaction cross sections in the low energy domain, $T_\pi \leqslant 250$ MeV. The dotted curve, the dashed curve, and the solid curve represent, respectively, the calculations of $O(q)$, $O(q^2)$, and $O(q^3)$. Experimental data are taken from Refs. [1–25].
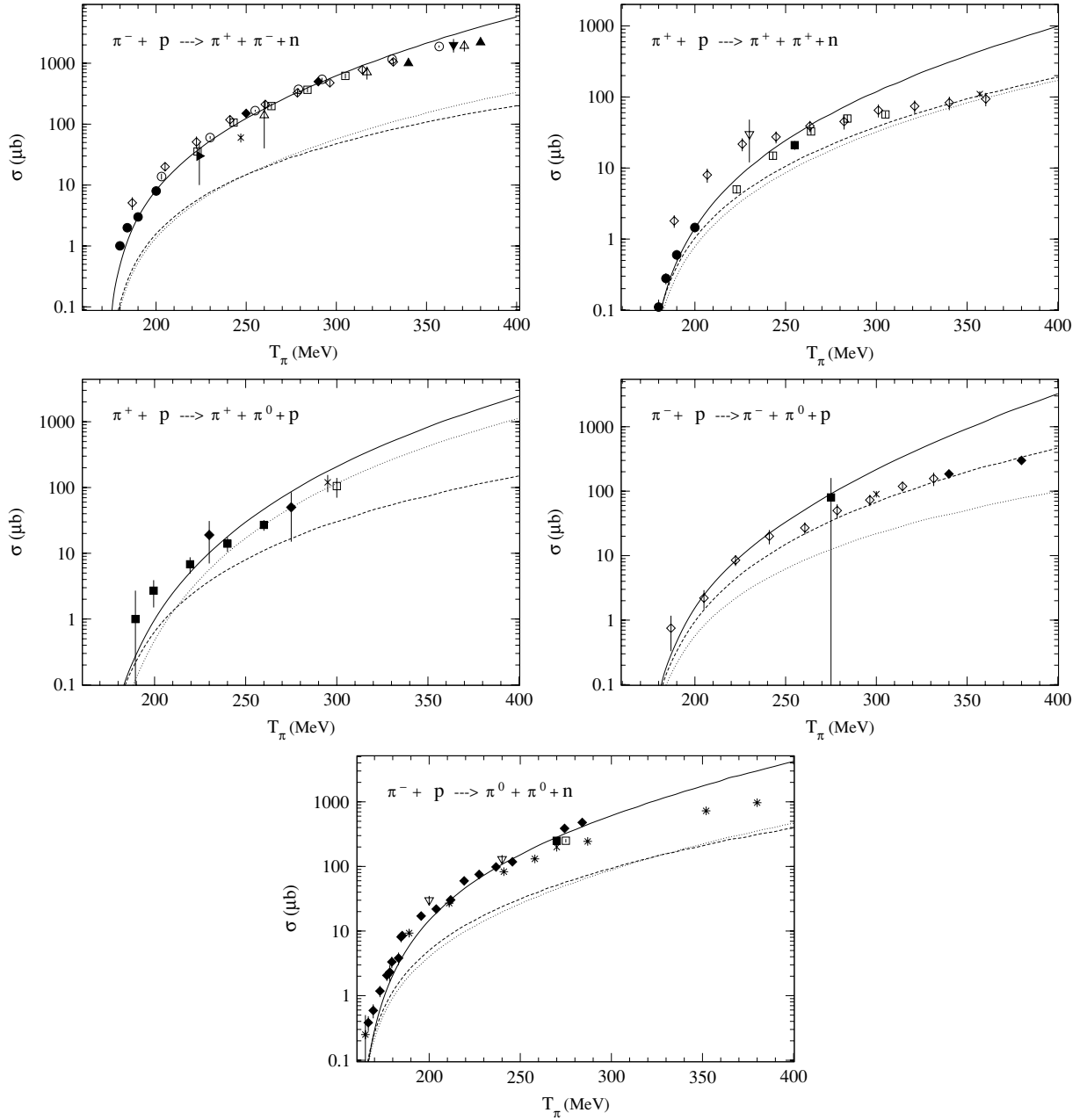
FIG. 3. Predictions for reaction cross sections up to $T_\pi = 400$ MeV. For notation see Fig. 2. Experimental data are taken from Refs. [1–25].

where u and u_v denote the Dirac and the heavy baryon spinors, respectively, and Γ and $\hat{\Gamma}$ are operators acting on appropriate spinors. The relation between the spinors u and u_v is given by

$$u(p) = \frac{\not{p} + M}{E + M} u_v(p). \quad (25)$$

The matching condition (24) holds in any reference frame due to the Lorentz invariance of the formalism. A particularly convenient choice for practical calculations is the initial nucleon rest frame (INRF) defined as [61]

$$p_i = Mv, \quad p_f = p_i + Q = Mv + Q. \quad (26)$$

For the reaction, we set $Q = q - q_1 - q_2$. Using Eq. (25) and after some straightforward calculations, we find that the matching condition (24) in the INRF results in the translation Table VII, with $C = 1 - Q^2/4M^2$.

The HBχPT amplitude for the reaction $\pi + N \to 2\pi + N$ (19) is given by Eq. (20), with the explicit tensor structures [Eqs. (22) and (23)]. The relativistic amplitude for the same reaction is parametrized as [31,32]

$$\mathcal{T}_{fi} = \bar{u}(p_f)\gamma_5[f_1 + f_2 \not{q}_1 + f_3 \not{q}_2 + f_4 \not{q}_1 \not{q}_2]u(p_i). \quad (27)$$

Use of Table VII, along with the matching condition (24), results in the following relations between the relativistic and

TABLE VII. Translation table of Γ and $\hat{\Gamma}$ for the $\pi + N \to 2\pi + N$ reaction.

Γ	$\hat{\Gamma}$
1	1
γ_5	$\dfrac{(q - q_1 - q_2) \cdot S}{MC}$
$\gamma_5 \not{q}_1$	$\dfrac{1}{MC}\{-S \cdot q_1(2MC + v \cdot q_1) - S \cdot q_2 v \cdot q_1 + S \cdot q v \cdot q_1\}$
$\gamma_5 \not{q}_2$	$\dfrac{1}{MC}\{-S \cdot q_1 v \cdot q_2 - S \cdot q_2(2MC + v \cdot q_2) + S \cdot q v \cdot q_2\}$
$\gamma_5 \not{q}_1 \not{q}_2$	$\dfrac{1}{MC}\Big\{-S \cdot q_1\big(2Mv \cdot q_2 + q \cdot q_2 - m_\pi^2\big)$ $+ S \cdot q_2\big(2Mv \cdot q_1 + q \cdot q_1 - m_\pi^2 - 2q_1 \cdot q_2\big)$ $+ S \cdot q q_1 \cdot q_2 + \dfrac{i}{2}\,\epsilon_{\mu\nu\alpha\beta} v^\alpha q^\beta q_1^\mu q_2^\nu\Big\}$

heavy-baryon structures:

$$f_1 = M\left(1 - \frac{t}{4M^2}\right)(A_0 - 2Bq_1 \cdot q_2) + \frac{1}{2}(A_0 + A_1)v \cdot q_1$$
$$+ \frac{1}{2}(A_0 + A_2)v \cdot q_2 + [v \cdot q_1 q \cdot q_2 - v \cdot q_2 q \cdot q_1$$
$$+ v \cdot (q_2 - q_1)(m_\pi^2 + q_1 \cdot q_2)]B, \tag{28}$$

$$f_2 = -\tfrac{1}{2}(A_0 + A_1) - \big[2Mv \cdot q_2 + q_2 \cdot (q - q_1) - m_\pi^2\big]B, \tag{29}$$

$$f_3 = -\tfrac{1}{2}(A_0 + A_2) + \big[2Mv \cdot q_1 + q_1 \cdot (q - q_2) - m_\pi^2\big]B, \tag{30}$$

$$f_4 = 2M\left(1 - \frac{t}{4M^2}\right)B. \tag{31}$$

It is important to note that these relations are valid to all orders in perturbation theory. In this work, however, the HBχPT amplitudes are calculated only up to order $O(q^3)$. If we use the threshold kinematics along with the explicit form of the Dirac spinor, Eq. (27) becomes

$$\mathcal{T}_{fi} = \frac{1}{2M} \chi^{(\alpha_f)\dagger}\big[-f_1 + m_\pi(f_2 + f_3) - m_\pi^2 f_4\big]\boldsymbol{\sigma} \cdot \boldsymbol{q} \chi^{(\alpha_i)}$$
$$\equiv a \chi^{(\alpha_f)\dagger} \boldsymbol{\sigma} \cdot \boldsymbol{q} \chi^{(\alpha_i)}, \tag{32}$$

TABLE VIII. Calculated values of D_1 and D_2.

	$O(q)$	$O(q^2)$	$O(q^3)$
$D_1(\text{fm}^3)$	2.50	2.14	1.90 ± 0.33
$D_2(\text{fm}^3)$	-7.70	-6.96	-11.44 ± 2.11

where

$$a = \frac{1}{2M}\big[m_\pi(f_2 + f_3) - f_1 - m_\pi^2 f_4\big]. \tag{33}$$

The quantity a is commonly referred to as the threshold amplitude. Let a_0 and a_+, represent the amplitudes for the reactions $\pi^- p \to \pi^0 \pi^0 n$ and $\pi^+ p \to \pi^+ \pi^+ n$, respectively. It is shown that near the reaction threshold, where only S and P partial waves make significant contributions, the isospin decomposition of the threshold amplitudes yields

$$a_0 = \frac{2}{3}\frac{1}{\sqrt{5}}a^{3,2} + \frac{\sqrt{2}}{3}a^{1,0}, \quad \text{and} \quad a_+ = \frac{2}{\sqrt{5}}a^{3,2}, \tag{34}$$

where a^{2I, I_π} denote the amplitude for a reaction channel having a total isospin I and the di-pion isospin I_π. The information about the $\pi\pi$ interaction in a well defined isospin channel is contained in the isospin amplitudes [62,63]. The relations between a^{2I, I_π} and the threshold isospin amplitudes D_1 and D_2 introduced in Ref. [34] are given as

$$D_1 = \frac{1}{\sqrt{10}}a^{3,2} = \frac{1}{2\sqrt{2}}a_+, \tag{35}$$

$$D_2 = -\frac{2}{3}\frac{a^{3,2}}{\sqrt{10}} - \frac{1}{3}a^{1,0} = -\frac{1}{\sqrt{2}}a_0. \tag{36}$$

In brief, our calculations include the following steps. We first compute the HBχPT amplitudes A_0, A_1, A_2, and B. Substitution of these amplitudes into Eqs. (28)–(31) yields the invariant amplitudes f_1, f_2, f_3, and f_4. Finally, we use Eq. (33) to obtain the threshold reaction amplitudes a_0 and a_+ from a knowledge of f_1, f_2, f_3, and f_4. Our numerical results for D_1 and D_2 up to chiral order $O(q^3)$ are listed in Table VIII. A notable feature of these results is the large contribution of
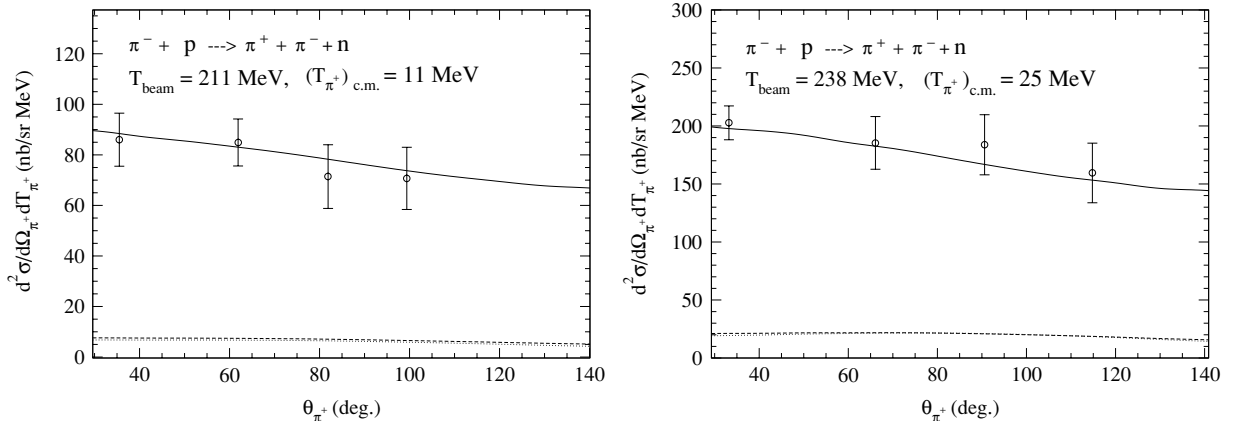

FIG. 4. Sample fits to double differential cross section data. For legends see Fig. 2. Experimental data from Refs. [26,27].
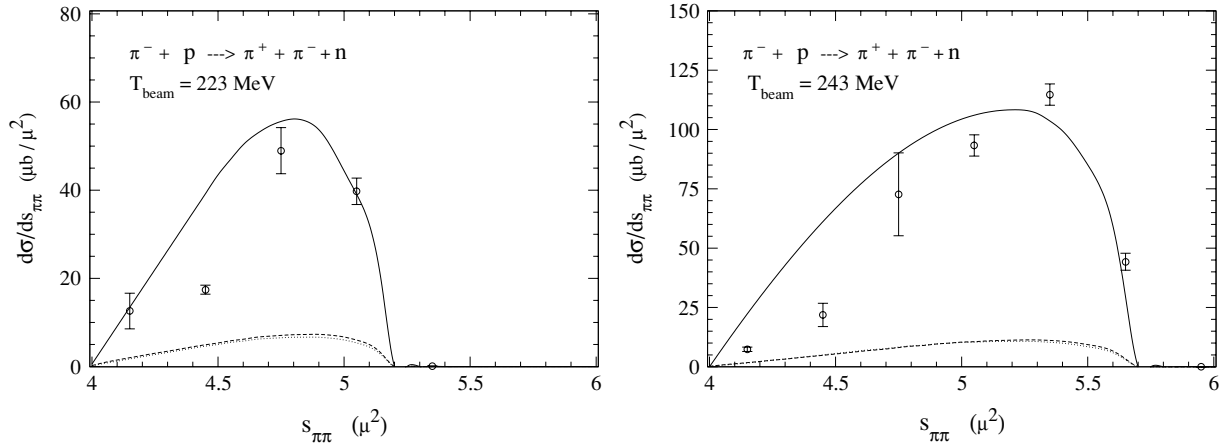
FIG. 5. Sample predictions for the differential cross section $d\sigma/ds_{\pi\pi}$. Here, $s_{\pi\pi}$ is the square of the invariant dipion mass in the final state measured in units of $\mu^2 = 4m_\pi^2$. For legend see Fig. 2. Data are from Refs. [23,24].

the nonleading terms to the amplitude D_2. A comparison of our results with the experimental data and with the results of previous theoretical works is presented in Table IX. Our results should be compared with HBχPT calculations of Ref. [34] which are in very good agreement with the data. We believe that the difference between the two sets of calculations is partially due to different truncation schemes employed at the amplitude level (as discussed in Sec. IV), and partially due to using different values of LECs of $O(q^3)$. Finally, we note that the calculations in Ref. [31], while not fully consistent with the power counting scheme of chiral perturbation theory, yield results which are in reasonable agreement with experimental data.

D. Unitarity Effects

Unitarity of the S-matrix requires that, in general, the S-matrix elements be complex. In a perturbative evaluation of the S-matrix, the tree diagrams are purely real, whereas the loop diagrams are generally complex. Therefore, the imaginary part of the scattering amplitude for a given process originates entirely from the loop diagrams. In HBχPT, the loop diagrams first set in at order $O(q^3)$. The loop diagrams of order $O(q^3)$ involve vertices from the lowest order Lagrangians $\mathcal{L}_{\pi N}^{(1)}$ and $\mathcal{L}_{\pi}^{(2)}$ with accurately determined LECs: g_A and F_π. Hence, the imaginary parts of the amplitudes of $O(q^3)$ can be viewed as parameter-free predictions of our calculations. Our calculated values of the threshold invariant amplitudes are listed in Table X. We find that the imaginary parts of

the amplitudes are generally non-negligible, and in certain instances are comparable with the real parts.

It is desirable to compare the parameter-free predictions of our loop-level calculations with the previous work in HBχPT for the reaction under consideration. That information is not available in the literature. For completeness sake, however, we make a few remarks about the tree-level calculations in Ref. [31]. As mentioned before, the calculation of Ref. [31] is not fully consistent with the chiral power counting scheme. There, the imaginary parts of the amplitudes are generated entirely by the width of the intermediate-state nucleon resonances. The findings of Ref. [31] may be summarized by saying that the imaginary parts of the amplitudes are sizable and play a significant role in providing a reasonable fit to the various observables considered.

E. Polarization observables

There are at least two motives for studying polarization observables for the reaction $\pi + N \to 2\pi + N$. First, accurate extraction of threshold amplitudes from experimental data requires disentanglement of different spin structures in the reaction amplitude. The unpolarized cross section measurements have limitations in this regard [36]. Furthermore, one may expect that the amplitude-selective nature of polarization observables may provide additional constraints for determination of the LECs of the theory. A theoretical investigation of the polarization observables based on phenomenological scattering amplitudes for the reaction $\pi + N \to 2\pi + N$ was carried out in Ref. [36]. Our calculations are performed in HBχPT. For the polarized target, the square modulus of the transition amplitude summed over appropriate nucleon spin degrees of freedom in the initial and final states can be written as

$$|\mathcal{T}_{fi}|^2 = \sum_{\alpha_i,\alpha_f} \left| \bar{u}_v^{(\alpha_f)}(p_f)\Sigma_v(n)\mathcal{A}u_v^{(\alpha_i)}(p_i) \right|^2, \quad (37)$$

TABLE IX. Values of D_1 and D_2.

	Experiment [65]	Present work	Theory [34]	Theory [31]
$D_1(\text{fm}^3)$	2.26 ± 0.12	1.90 ± 0.33	2.65 ± 0.24	1.87
$D_2(\text{fm}^3)$	-9.05 ± 0.36	-11.44 ± 2.11	-9.06 ± 1.05	-10.58

TABLE X. Numerical values of f_1, f_2, f_3, and f_4 at threshold.

Channel	$O(q^n)$	f_1/m_π^2	f_2/m_π^3	f_3/m_π^3	f_4/m_π^4
$\pi^- + p \rightarrow \pi^0 + \pi^0 + n$	$O(q)$	-44.30	3.90	3.90	0
	$O(q^2)$	-39.51	3.81	3.81	0
	$O(q^3)$	$-38.69 + i\,47.88$	$3.20 - i5.22$	$3.20 - i5.22$	0
$\pi^+ + p \rightarrow \pi^+ + \pi^+ + n$	$O(q)$	30.75	-1.44	1.44	0
	$O(q^2)$	25.36	-1.71	1.71	0
	$O(q^3)$	$-23.71 - i3.89$	$1.67 + i0.03$	$1.67 + i0.03$	0

where $\mathcal{A}$ is given by Eq. (22), $u_v^{(\alpha)}$ denotes a heavy baryon spinor with a polarization label α, $\Sigma_v(n)$ is a spin projection operator

$$\Sigma_v(n) = \frac{1 + 2S_v \cdot n}{2}, \qquad (38)$$

with n_μ a unit space-like polarization four-vector, and S_v the spin operator given by Eq. (6). In the target rest frame, $n^\mu = (0, \boldsymbol{n})$, and Σ_v reduces to $(1 + \boldsymbol{\sigma} \cdot \boldsymbol{n})/2$. Using explicit expressions for $\mathcal{T}$ given by Eqs. (22) and (23), straightforward calculation results in the following expression for the square modulus of the transition amplitude:

$$
\begin{aligned}
|\mathcal{T}_{fi}|^2 = C(p_i)C(p_f) \times \Bigg(&+\frac{1}{4}[|A \cdot v|^2 - |A|^2] \\
&+ \epsilon_{\alpha\beta\mu\nu}\epsilon_{abcd}v^\alpha v^a q^\beta q^b q_1^\mu q_1^c q_2^\nu q_2^d |B|^2 \\
&+ \epsilon_{\alpha\beta\mu\nu}\Big(v^\alpha q^\beta q_1^\mu q_2^\nu \mathrm{Im}[(n \cdot A)^* B] - v^\alpha q^\beta q_1^\mu q_2^\nu (v \cdot n) \\
&\times \mathrm{Im}[(v \cdot A)^* B] + \frac{i}{4} v^\alpha n^\beta A^\mu (A^\nu)^* \Big) \Bigg),
\end{aligned} \qquad (39)
$$

where $C(p) \equiv (v \cdot p + M/2M) = 1$ on the mass shell. The first two line in Eq. (39) correspond to the unpolarized target, whereas the remaining two lines represent contributions due to the target polarization. As one might expect, polarization effects are manifested as the interference between real and imaginary parts of the transition amplitude. In HBχPT the imaginary part of an amplitude originates entirely from loop diagrams. Therefore, one obtains nonvanishing results for polarization observables only at $O(q^3)$ and beyond. Following Ref. [36], we define an asymmetry as

$$A_{\mathbf{xy}}(\phi_{\mathbf{z}}) \equiv \frac{\sigma(\phi_{\mathbf{z}}) - \sigma(-\phi_{\mathbf{z}})}{\sigma(\phi_{\mathbf{z}}) + \sigma(-\phi_{\mathbf{z}})}, \qquad (40)$$

where $\mathbf{x}$, $\mathbf{y}$, $\mathbf{z}$ are three (not necessarily orthogonal) vectors. The angle $\phi_{\mathbf{z}}$ is the azimuthal angle of $\mathbf{z}$ in a plane which contains $\mathbf{y}$ and is orthogonal to $\mathbf{xy}$-plane. A comprehensive list of asymmetries for the reaction $\pi + N \rightarrow 2\pi + N$ is given in Ref. [36], wherein it was predicted that, for the transverse polarization of the target all but two observables, $A_{\mathbf{n},\mathbf{p}}(\phi_{\mathbf{q}})$ and $A_{\mathbf{n},\mathbf{q}}(\phi_{\mathbf{p}})$, are small. Here, $\mathbf{n}$ is the unit polarization vector for the target proton, $\mathbf{q}$ is the momentum of the incoming pion beam, and $\mathbf{p}$ is the momentum of the final-state nucleon.[2] Our calculations in HBχPT show that all asymmetries are small (i.e., $A_{\mathbf{xy}}(\phi_{\mathbf{z}}) \leqslant 0.4$). Our result for the observable $A_{\mathbf{n},\mathbf{p}}(\phi_{\mathbf{q}})$ is shown in Fig. 8. While the qualitative trend of our calculation is same as that reported in Ref. [36], our quantitative prediction is smaller by a factor of 2 to 3 over the angular range considered. Furthermore, we find that our results are not sensitive to moderate changes in the values of LECs. Polarization measurements for the reaction under consideration have been recently performed at TRIUMF. The analysis of experimental data is in progress [54].

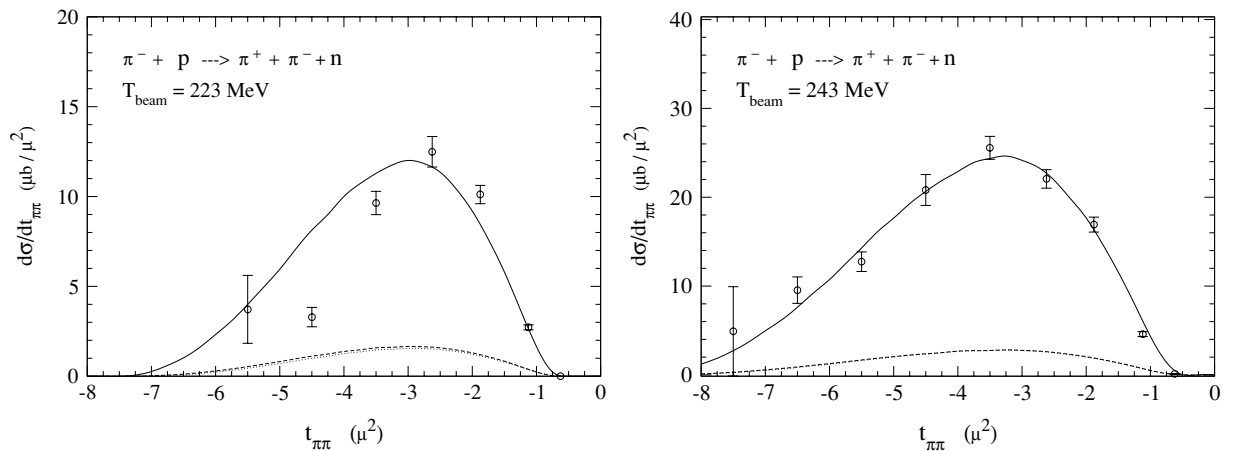[2]The two observables are connected by a symmetry relation.

FIG. 6. Sample predictions for the differential cross section $d\sigma/dt_{\pi\pi}$. Here, $t_{\pi\pi}$ is the invariant t-channel momentum transfer squared for the final state dipion. The quantity $t_{\pi\pi}$ is measured in units of $\mu^2 = 4m_\pi^2$. For legend see Fig. 2. Data are from Refs. [23,24].
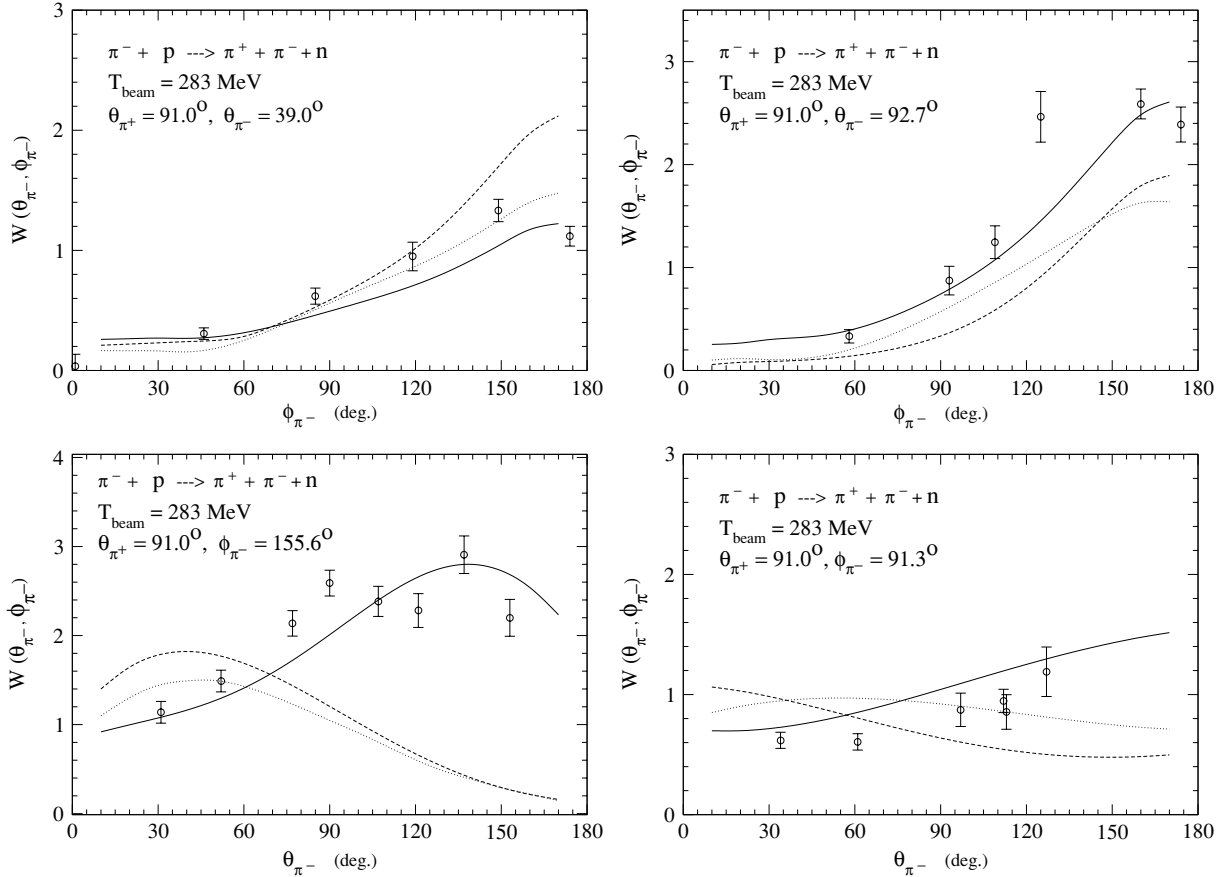
FIG. 7. Sample predictions for the angular correlation function at different kinematic domains. For legend see Fig. 2. Data are from Ref. [28].

IV. A COMPARISON BETWEEN TRUNCATION SCHEMES

Our calculations and those of Refs. [34,38] are carried out in HBχPT of $O(q^3)$. There are, however, some quantitative differences between the two sets of results which can be understood as follows. Let us first consider the threshold amplitudes D_1 and D_2. Consider the tree-level pion pole diagram of $O(q)$ contributing to the reaction $\pi^-(q) + p(p_i) \rightarrow \pi^0(q_1) + \pi^0(q_2) + n(p_f)$ where the pion and the pion-nucleon vertices are taken, respectively, from $\mathcal{L}_\pi^{(2)}$ and $\mathcal{L}_{\pi N}^{(1)}$. The pion propagator has chiral order -2. Therefore, according to the standard counting rules, we regard the diagram as having chiral order one ($1 = 2 + 1 - 2$). In our notation, after a brief calculation, the center-of-mass threshold transition amplitude for the above mentioned diagram takes on the form

$$\mathcal{T}_{fi} = -\frac{\sqrt{2}}{12}\left(\frac{g_A}{F^3}\right)\left(\frac{4q_0 + 5m_\pi}{q_0 - m_\pi}\right)$$
$$\times \bar{u}_v(p_f)(S \cdot q)u_v(p_i)) \equiv O(q), \quad (41)$$

Here, q_0 is the total energy of the incoming pion at the reaction threshold and is given by

$$q_0 = \frac{5m_\pi^2 + 4m_\pi m_N}{2(2m_\pi + m_N)}. \quad (42)$$

Now, one may further expand Eq. (41) in powers of $(m_\pi/m_N) \equiv O(q)$ to obtain

$$\mathcal{T}_{fi} = -\sqrt{2}\left(\frac{13}{12}\right)\left(\frac{g_A}{F^3}\right)\bar{u}_v(S \cdot q)u_v - \sqrt{2}\left(\frac{27}{24}\right)\left(\frac{g_A}{F^3}\right)$$
$$\times \left(\frac{m_\pi}{m_N}\right)\bar{u}_v(S \cdot q)u_v - \frac{\sqrt{2}}{12}\left(\frac{g_A}{F^3}\right)O\left(\geqslant\frac{m_\pi^2}{m_N^2}\right)$$
$$\times \bar{u}_v(S \cdot q)u_v = O(q) + O(q^2) + O(\geqslant q^3) \overset{O(q)}{=}$$
$$-\sqrt{2}\left(\frac{13}{12}\right)\left(\frac{g_A}{F^3}\right)\bar{u}_v(S \cdot q)u_v. \quad (43)$$

We regard Eq. (41) as an amplitude of $O(q)$, whereas in Refs. [33,34] the additional expansion in m_π/m_N is carried out and Eq. (43) is defined as an amplitude of $O(q)$. We have verified that when all the pertinent diagrams up to $O(q^3)$ are taken into account and expansion in m_π/m_N is carried out, our analytical results for the threshold amplitudes D_1 and D_2 coincides with those given in Refs. [33,34].[3] In general, however, once a diagram is identified as having a

---

[3]Note that the expansion of D_1 and D_2 up to $O((m_\pi/m_N)^2)$ corresponds to chiral expansion of $O(q^3)$. This is because according to the counting scheme of Refs. [33,34] terms of $O(q)$ in D_1 and D_2 are of zeroth order in m_π/m_N.
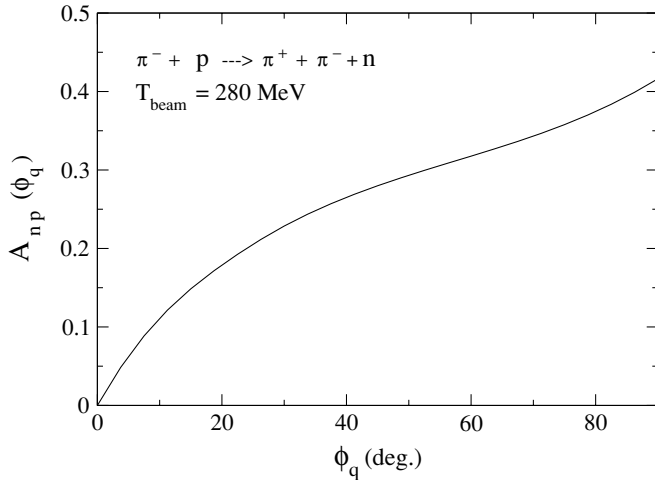
FIG. 8. Theoretical prediction for the asymmetry parameter $A_{np}(\phi_q)$. For additional details see the text.

fixed chiral order, we do not further expand the corresponding amplitude to generate a chiral series of higher order. As for the numerical values of D_1 and D_2, there are additional sources of difference between our results and those of Ref. [34]. In Ref. [34] the relevant LECs of $O(q^2)$ were fixed such that they are consistent with the low energy theorem for pion-nucleon scattering at $O(m_\pi/m_N)$. Furthermore, in Ref. [34] the resonance saturation method was employed to estimate the values of LECs of $O(q^3)$. In the present work the LECs of $O(q^2)$ are taken from Ref. [53] where they are determined by fitting the low energy pion-nucleon scattering data. As for the unknown LECs of $O(q^3)$, in the present work they are fixed by fitting the low energy total and double differential cross section data as discussed in Sec. III.

Let us now consider various types of cross sections above the reaction threshold. In Ref. [38], in contrast with Ref. [34], the additional expansion of amplitudes in m_π/m_N is not carried out. As such, our results should formally coincide with those reported in Ref. [38]. Beyond the threshold there is a substantial increase in the number of Feynman diagrams, and in addition, a number of loop integrations cannot be performed analytically. Furthermore, the phase space calculations for different observables are performed numerically. As such, a comparison between our results and those of Ref. [38] cannot be made at an analytical level. We ascribe the small quantitative difference between the two sets of results predominantly to using different values of LECs, with the numerical aspects of various integrations accounting for the remaining difference.

V. SUMMARY AND CONCLUSIONS

We divide our conclusions into two broad categories of comparison between theory and experiment, and theoretical issues. Let us consider each category in turn.

A. Comparison with experiment

(i) The reaction cross sections are in reasonable agreement with experimental data with better results at lower energies. This is to be expected, given that HBχPT is a low energy theory, and that the unknown LECs are fitted to the low energy data.

(ii) The double differential cross sections $d^2\sigma/d\Omega dT$ included in the fitting procedure are reproduced well. The remaining differential cross-sections, $d\sigma/ds$ and $d\sigma/dt$, and angular correlations, $W(\theta, \phi)$, which can be regarded as parameter-free results of the present calculations, are reproduced semiquantitatively.

(iii) Our results for threshold amplitudes D_1 and D_2 are in fair, but not impressive, agreement with data.

(iv) Our predictions for polarization observables (asymmetries) are generally small ($\leqslant 0.4$). If in the final experimental analysis the asymmetries turn out to be indeed small, then a precise extraction of $\pi\pi$-scattering lengths from $\pi + N \to 2\pi + N$ reactions may prove difficult.

B. Theoretical issues

(i) In general, physical observables calculated in this work receive sizable contributions from amplitudes of $O(q^3)$. These contributions are essential for quantitative agreement with the data. The large amplitudes of $O(q^3)$ originate from a number of loop graphs, and also from graphs involving large LECs of $O(q^3)$. It should be emphasized that some LECs of $O(q^3)$ determined in this work are larger than their expected natural size.

(ii) We have explicitly calculated the unitarity effects for two reaction channels $\pi^- + p \to \pi^0 + \pi^0 + n$ and $\pi^+ + p \to \pi^+ + \pi^+ + n$ at the reaction threshold. The unitarity effects appear to be sizable. The unitarity corrections are essentially parameter-free in that they only involve precisely determined LECs of $O(1)$.

(iii) There is a large overlap between present work and those reported in Refs. [34,38]. The results and conclusions are in broad agreement. There are, however, small quantitative differences between the two sets of results. So far as threshold amplitudes D_1 and D_2 are concerned, the quantitative differences between our results and those of Ref. [34] are fully understood. The differences are due to different truncation schemes employed as well as using different values for LECs of $O(q^2)$ and of $O(q^3)$. Let us now consider the results above the reaction threshold. To facilitate a comparison between the two sets of results we have used the same fitting criteria for the LECs of $O(q^3)$ as those employed in Ref. [38]. We have arrived at somewhat different values for the LECs. Because of the numerical aspects of the calculations above the reaction threshold, a direct analytical comparison between the two sets of results is not possible. We attribute the small differences above the reaction threshold almost entirely to using different values for LECs of $O(q^3)$. Approximations inherent in numerical algorithms for performing phase space integrations also contribute a small amount to the difference in the results.

Chiral perturbation theory is the effective low energy theory of QCD. As such, the short distance dynamics of QCD are encoded in the LECs of chiral perturbation theory. For the energy scales under consideration, the values of the

LECs of the theory can be understood semiquantitatively in terms of "heavy" hadronic degrees of freedom such as low-lying mesonic and baryonic resonances [66]. The sizable contributions at $O(q^3)$ may suggest that certain aspects of short distance physics (heavy degrees of freedom), not explicitly taken into account in the chiral Lagrangian but implicitly included in the LECs, play an important role in the reaction under study at $O(q^3)$. If the essence of the short distance physics for the reaction under consideration is captured at $O(q^3)$, it is then conceivable that beyond $O(q^3)$ the chiral series may become well behaved. That is, contributions of $O(q^4)$ or higher may become noticeably suppressed compared to those of $O(q^3)$. This conjecture can be explicitly verified only if calculations of $O(q^4)$ are performed. It is worth mentioning that the complete one-loop analysis in HBχPT requires a calculation of $O(q^4)$. A different, but equally illuminating, approach is to include the low-lying resonances as dynamical degrees of freedom in the formalism and explore their consequences. The small-scale expansion is an example of this approach [67].

We conclude by stating that HBχPT, in its standard form, appears to be a slowly converging series for the reaction $\pi + N \rightarrow 2\pi + N$. The reaction $\pi + N \rightarrow 2\pi + N$ is an important source of information about $\pi\pi$ scattering. As such, it is perhaps worthwhile to study this reaction in alternative formulations of BχPT, in order to further explore the convergence properties of the chiral series [45,46,68–70].

ACKNOWLEDGMENT

[1] M. Sevior *et al.*, Phys. Rev. Lett. **66**, 2569 (1991).

[2] G. Kernel *et al.*, Phys. Lett. **B216**, 244 (1989); **B225**, 198 (1989).

[3] G. Kernel *et al.*, Z. Phys. C **48**, 201 (1990).

[4] J. Kirz, J. Schwartz, and R. D. Tripp, Phys. Rev. **126**, 763 (1962).

[5] D. Pocanić *et al.*, Phys. Rev. Lett. **72**, 1156 (1994).

[6] M. Arman *et al.*, Phys. Rev. Lett. **29**, 962 (1972).

[7] Yu. A. Batsuov *et al.*, Sov. J. Nucl. Phys. **1**, 374 (1965).

[8] Yu. A. Batsuov *et al.*, Sov. J. Nucl. Phys. **21**, 162 (1975).

[9] T. D. Blokhintseva *et al.*, Sov. Phys. JETP **17**, 340 (1963).

[10] A. A. Bel'kov *et al.*, Sov. J. Nucl. Phys. **28**, 657 (1978).

[11] A. A. Bel'kov *et al.*, Sov. J. Nucl. Phys. **31**, 96 (1980).

[12] S. A. Bunyatov *et al.*, Sov. J. Nucl. Phys. **25**, 177 (1997).

[13] A. V. Kratsov *et al.*, Sov. J. Nucl. Phys. **20**, 500 (1975).

[14] V. Barnes *et al.*, CERN Report 63-67, 1963.

[15] C. W. Bjork *et al.*, Phys. Rev. Lett. **44**, 62 (1980).

[16] J. A. Jones, W. W. M. Allison, and D. H. Saxon, Nucl. Phys. **B83**, 93 (1974).

[17] I. M. Blair *et al.*, Phys. Lett. **B32**, 528 (1970).

[18] D. H. Saxon, J. M. Mulvey, and W. Chinowsky, Phys. Rev. D **2**, 1790 (1970).

[19] J. Deahl *et al.*, Phys. Rev. **124**, 1987 (1961).

[20] W. A. Perkins *et al.*, Phys. Rev. **118**, 1364 (1960).

[21] J. Lowe *et al.*, Phys. Rev. C **44**, 956 (1991).

[22] S. Prakhov *et al.*, Phys. Rev. C **69**, 045202 (2004).

[23] M. Kermani *et al.*, Phys. Rev. C **58**, 3419 (1998).

[24] M. Kermani, Ph.D. thesis, "Exclusive Measurments of $\pi + N \rightarrow 2\pi + N$," The University of British Columbia, 1997.

[25] J. B. Lange *et al.*, Phys. Rev. Lett. **80**, 1597 (1998).

[26] D. M. Manley, Phys. Rev. D **30**, 536 (1984).

[27] D. M. Manley, R. A. Arndt, Y. Goradia, and V. L. Teplitz, Phys. Rev. D **30**, 904 (1984).

[28] R. Müller *et al.*, Phys. Rev. C **48**, 981 (1993).

[29] E. Oset and M. J. Vicente-Vacas, Nucl. Phys. **A446**, 584 (1985).

[30] O. Jäkel, H. W. Ortner, M. Dillig, and C. A. Z. Vasconcellos, Nucl. Phys. **A511**, 733 (1990); O. Jäkel, M. Dilling, and C. A. Z. Vasconcellos, *ibid.* **A541**, 675 (1992); O. Jäkel and M. Dillig, *ibid.* **A561**, 557 (1993).

[31] T. S. Jensen, πN Newsletter **10**, 179, (1995); T. S. Jensen and A. F. Miranda, Phys. Rev. C **55**, 1039 (1997).

[32] J. Beringer, πN Newsletter **7**, 33 (1992).

[33] V. Bernard, N. Kaiser, and Ulf-G. Meißner, Phys. Lett. **B332**, 415 (1994).

[34] V. Bernard, N. Kaiser, and Ulf-G. Meißner, Nucl. Phys. **B457**, 147 (1995).

[35] V. Bernard, N. Kaiser, and Ulf-G. Meißner, Nucl. Phys. **A619**, 261 (1997).

[36] A. A. Bolokhov, V. A. Kozhevnikov, D. N. Tatarkin, and S. G. Sherman, Phys. Rev. C **61**, 055203 (2000).

[37] J. Zhang, N. Mobed, and M. Benmerrouche, nucl-th/9806063.

[38] N. Fettes, V. Bernard, and Ulf-G. Meißner, Nucl. Phys. **A669**, 269 (2000).

[39] J. Gasser, M. E. Sainio, and A. Švarc, Nucl. Phys. **B307**, 779 (1988).

[40] A. Krause, Helv. Phys. Acta **63**, 3 (1990).

[41] E. Jenkins and V. Manohar, Phys. Lett. **B255**, 558 (1991).

[42] P. J. Ellis and H. B. Tang, Phys. Rev. C **57**, 3356 (1998).

[43] J. Gegelia and G. Japaridze, Phys. Rev. D **60**, 114038 (1999).

[44] M. Lutz, Nucl. Phys. **A677**, 241 (2000).

[45] T. Becher and H. Leutwyler, Eur. Phys. J. C **9**, 643 (1999); J. High Energy Phys. 06 (2001) 017.

[46] T. Fuchs, J. Gegelia, G. Japaridze, and S. Scherer, Phys. Rev. D **68**, 056005 (2003).

[47] K. Torikoshi and P. J. Ellis, Phys. Rev. C **67**, 015208 (2003).

[48] C.-W. Kao, B. Pasquini, and M. Vanderhaeghen, Phys. Rev. D **70**, 114004 (2004).

[49] B. C. Tiburzi, Phys. Rev. D **71**, 034501 (2005) and references cited therein.

[50] V. Bernard, N. Kaiser, and Ulf-G. Meißner, Int. J. Mod. Phys. E **4**, 193 (1995).

[51] G. Ecker, Prog. Part. Nucl. Phys. **35**, 1 (1995).

[52] S. Scherer, in *Advances in Nuclear Physics*, Vol. 27, p. 277 (Kluwer Academic/Plenum Publishers, New York, 2003).

[53] M. Mojzis, Eur. Phys. J. C **2**, 181 (1998).

[54] Private communication with CHAOS collaboration on the analysis of the TRIUMF experiment E862.

[55] G. Ecker and M. Mojzis, Phys. Lett. **B365**, 312 (1996).

[56] N. Fettes, Ulf-G. Meißner, and S. Steininger, Nucl. Phys. **A640**, 199 (1998).

[57] H. W. Fearing, R. Lewis, N. Mobed, and S. Scherer, Phys. Rev. D **56**, 1783 (1997).

[58] Particle Data Group, R. M. Barnett, C. D. Carone, D. E. Groom, T. G. Trippe, C. G. Wohl, B. Armstrong, P. S. Gee, G. S. Wagman,

F. James, M. Mangano, K. Monig, L. Montanet, J. L. Feng, H. Murayama, J. J. Hernandez, A. Manohar, M. Aguilar-Benitez, C. Caso, R. L. Crawford, M. Rocs, N. A. Tornqvist, K. G. Hayes, K. Hagiwara, K. Nakamura, M. Tanabashi, K. Olive, K. Honscheid, P. R. Burchat, R. E. Shrock, S. Eidelman, R. H. Schindler, A. Gurtu, K. Hikasa, G. Conforto, R. L. Workman, C. Grab, and C. Amsler, Phys. Rev. D **54**, 1 (1996).

[59] J. Zhang, "A Study of the Reaction $\pi + N \to 2\pi + N$ in Chiral Perturbation Theory," Ph.D. thesis, University of Regina, 1998.

[60] Y. Kim, F. Myhrer, and K. Kubodera, Prog. Theor. Phys. **112**, 289 (2004).

[61] G. Ecker and M. Mojzis, Phys. Lett. **B410**, 266 (1997).

[62] M. G. Olsson, Ulf-G. Meißner, N. Kaiser, and V. Bernard, πN Newsletter **10**, 201 (1995).

[63] M. G. Olsson, Phys. Lett. **B410**, 311 (1997).

[64] J. B. Lange *et al.*, πN Newsletter **13**, 32 (1997).

[65] H. Burkhardt and J. Lowe, Phys. Rev. Lett. **67**, 2622 (1991); πN Newsletter **8**, 173 (1993).

[66] J. F. Donoghue, C. Ramirez, and G. Valencia, Phys. Rev. D **39**, 1947 (1989); G. Ecker, J. Gasser, A. Pich, and E. de Rafael, Nucl. Phys. **B321**, 311 (1989); B. Kubis and Ulf.-G. Meißner, *ibid*. **A679**, 698 (2001).

[67] T. R. Hemmert, B. R. Holstein, and J. Kambor, J. Phys. G **24**, 1831 (1998); V. Bernard, T. R. Hemmert, and Ulf-G. Meißner, Nucl. Phys. **A686**, 290 (2001).

[68] J. F. Donoghue, B. R. Holstein, and B. Borasoy, Phys. Rev. D **59**, 036002 (1999); B. Borasoy, B. R. Holstein, R. Lewis, and P.-P. A. Ouimet, *ibid*. **66**, 094020 (2002).

[69] R. Lewis and Pierre-Philippe A. Ouimet, Phys. Rev. D **64**, 034005 (2001); B. Borasoy, R. Lewis, and Pierre-Philippe A. Ouimet, *ibid*. **65**, 114023 (2002).

[70] V. Bernard, T. R. Hemmert, and Ulf-G. Meißner, Nucl. Phys. **A732**, 149 (2004).